Propagation Characteristics of Air-to-Air Channels in Urban Environments

Lai Zhou[1], Zhi Yang[2], Guangyue Zhao[2], Shidong Zhou[2], and Cheng-Xiang Wang[3,4]

[1]Department of Engineering Physics, Tsinghua University, Beijing, China
[2]Department of Electronic Engineering, Tsinghua University, Beijing, China
[3]School of Information Science and Engineering, Southeast University, Nanjing, China
[4]School of Engineering and Physical Sciences, Heriot-Watt University, Edinburgh, UK
Email: {zhoulai13,yang-z15,zhaogy17}@mails.tsinghua.edu.cn, zhousd@mail.tsinghua.edu.cn, chxwang@seu.edu.cn

Abstract—In this paper, we study the propagation character-istics of air-to-air (A2A) channels in a virtual urban scenario generated with the ITU-R model. Based on ray-tracing sim-ulations, we explore the behavior of large-scale fading when taking the environmental setup into consideration. Our analytical results show that the large-scale fading statistics, e.g., pathloss exponent (PLE) and shadow fading variance, are associated with the receiver height and elevation angle. Furthermore, we derive an approximate expression for line-of-sight probability according to the deployment and distribution of buildings. The expression is characterized as a function of receiver height and elevation angle with the condition of high transmitter height. To efficiently evaluate the performance of unmanned aerial vehicle (UAV) communication systems, we then propose an empirical propagation channel prediction model, which can be easily extended to different scenarios in the ITU-R model.

Index Terms—UAV communications, air-to-air channels, ray-tracing, pathloss model, LOS probability.

I. INTRODUCTION

In recent years, UAV communications have attracted much attention due to their high mobility and low cost. Their typical applications include aerial photography, traffic monitoring, and disaster relief [1]. Considering less blockage and col-lision probability, most of the applications concentrate on the suburban and open area scenarios. Furthermore, with the development of artificial intelligence and system management, it is promising to support some amazing applications in urban environments, e.g., package delivery, aerial relay for device-to-device (D2D) communications, and aerial transportation [2]-[4]. The physical wireless channel has an important effect on the communication system, motivating us to focus on the channel property and challenge of UAV communication in an urban scenario.

A. Related work and Motivation

There are many application scenarios related to the A2A channel, e.g., cellular-to-UAV networks, D2D communication and *ad hoc* network. The A2A channel is more likely to experience LOS propagation at an open area, in which the PLE is almost 2 similar as the propagation in free space [5]. However, when considering the UAV at low altitude in urban environment, the multipath may dominate the channel due to blockage from nearby buildings. Also, the height plays an

important role in channel behavior since there is less blockage at a higher altitude.

The conventional ground-to-ground (G2G) models [11] in-clude Stanford University Interim (SUI) Model, COST-231 Hata Model and ECC-33 model, and some models (e.g., SUI model) also consider the impact of transmitter (TX) and receiver (RX) height. However, these empirical models are associated with the application scenario and are difficult to extend to the A2A channel. Recently, there have been several research papers about channel measurement and modeling for air-to-ground (A2G) channels. In rural and hilly scenario, [6] expressed that the PLE decreases with an increase in the TX height. In urban scenario, [7] proposed a simplified Saleh-Valenzuela (SV) model to express the multipath, and [8] reported that the elevation angle heavily influences the excess fading in the pathloss. Very few works critically investigate such properties in A2A channels.

The empirical result is strongly dependent on the corre-sponding environment. In order to obtain a reliable model in different scenarios, a large number of data needs to be gathered with the conventional channel measurement, which is a heavy and time consuming work. On the purpose of investigating the primary behavior of A2A channel, a good and simple approach is performed by ray-tracing simulation [9]. The virtual-city environment is generated based on the In-ternational Telecommunication Union (ITU-R) model [10], so that it is efficient to analyze and compare the channel property with different geometry and frequency. The simulation result provides a guideline for A2A channel, and the parameters should be validated by real data in the future measurement. The main contributions of this paper are listed below.

B. Contributions

1) propagation property for A2A channel: According to ray-tracing simulation, we expose a relationship between large-scale fading statistics and environmental setups, e.g., RX altitude and elevation angle, in the line-of-sight (LOS) and non-line-of-sight (NLOS) scenarios, respectively.

2) LOS probability for A2A channels: With the deployment and distribution of buildings, we derive an approximate expres-sion of LOS probability, which can be simplified as a function
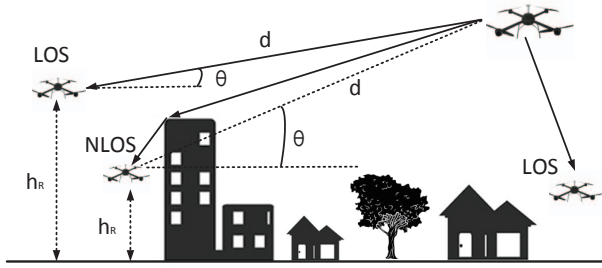
Fig. 1. A geometry of LOS and NLOS scenarios in an A2A channel.

of RX altitude and elevation angle with the assumption of high TX altitude.

3) Empirical propagation model: According to conventional pathloss model, we propose an empirical model for A2A channels in an urban scenario, which is suitable for different geometry structure in the ITU-R model.

The remainder of the paper is organized as follows: In Section II we introduce the ray-tracing simulation environments, and Section III expresses the property of A2A channel and the numerical relationships. The approximation of LOS probability is derived in Section IV. Section V presents the implement guideline of the pathloss model and conducts the verification. Finally, Section VI concludes the paper.

II. SIMULATION ENVIRONMENTS

A. Modeling urban environments

Fig. 1 depicts the geometry of LOS and NLOS scenarios in the A2A channel. The UAV as TX is deployed at a certain high altitude, e.g., 300 m, to provide cellular coverage for the UAV as RX with a low altitude of h_R and an elevation angle of θ. Since the layout of the buildings determines the behavior of propagation channel inside a city, the building deployment to express different scenario is generated based on the following three empirical parameters in ITU-R model [10] :

1) α: The ratio of built-up land area to the total land area (dimensionless).
2) β: The mean number of buildings per unit area (buildings / km^2).
3) γ: The variable to represent the building heights in Rayleigh distribution as

$$f(h) = \frac{h}{\gamma^2} exp(-\frac{h^2}{2\gamma^2}) \qquad (1)$$

where $f(h)$ is the probability density function (PDF) and h is the building height in meters. For simplicity, the virtual-city environment is generated as

$$W = \sqrt{\frac{\alpha}{\beta}} \qquad (2)$$

$$S = \frac{1}{\sqrt{\beta}} - W \qquad (3)$$

where W is the width of square building and S is the inter-building spacing. In addition, the deployments of trees and mobile objects are neglected in our simulation scenario.
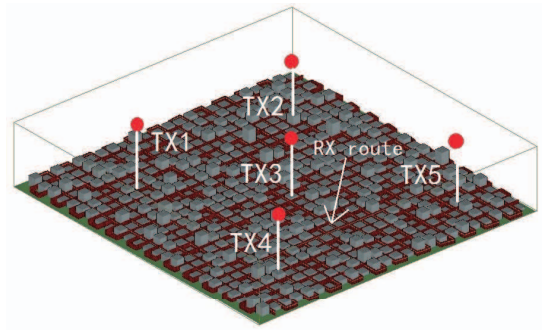

Fig. 2. A geographical scenario for ray-tracing simulations.

TABLE I
SIMULATION PARAMETERS.

Parameter	Value
Scenario	Dense urban, Urban
Simulation frequency	2.4 GHz, 800 MHz
Bandwidth	100 MHz
Simulation area	1.5 km $\times$ 1.5 km
TX height	300 m
RX height	2, 5, 10, 15, 20, 25, 30, 35, 40 m
RX spacing	5 m
Max. number of reflection	10
Max. number of penetration	Not simulated
Max. number of diffraction	1
Transmit power	0 dBm
Number of TXs	5
Number of RXs	14575 $\times$ 9
Minimum received power	-250 dBm

B. Simulation scenario

Fig. 2 depicts the geographical scenario with dimensions of 1.5 by 1.5 km. There are 5 TXs as red dots at a certain high altitude, and the RXs are deployed with 5 m resolution among the streets. It is important to note that the RXs are deployed at different heights to collect the signal power samples for the A2A channel. The maximum height of RX is 40 m, and most of the buildings are lower than such a height. Details of the simulation parameters are listed in Table I.

A full 3D ray-tracing simulation is performed with Wireless insite® software. The "Direct", "Reflected" and "Diffracted" paths are considered in our simulation, and the penetration path is neglected because of high attenuation through building. All the buildings are assumed to be made of concrete with $\epsilon_0 = 15$ and $\sigma_0 = 0.015$ [9], and the ground is assumed to be asphalt with $\epsilon_0 = 5.72$ and $\sigma_0 = 0.0005$ [9]. Isotropic rays are shoot from TXs with the power of 0 dBm and the threshold of received power is -250 dBm.

III. LARGE-SCALE FADING CHANNEL MODEL

The large-scale fading, or the pathloss, is the fundamental parameter to determine the coverage distance for cellular
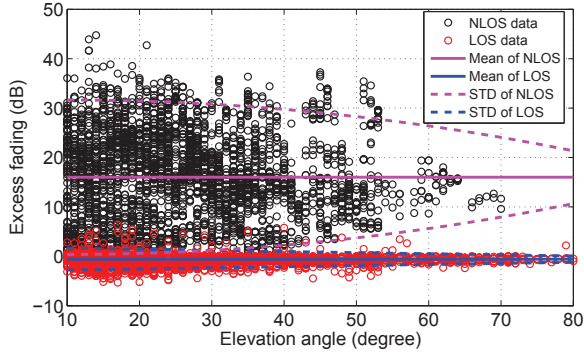
Fig. 3. Excess fading for the EL model in a dense urban scenario (RX = 30 m, f = 2.4 GHz).
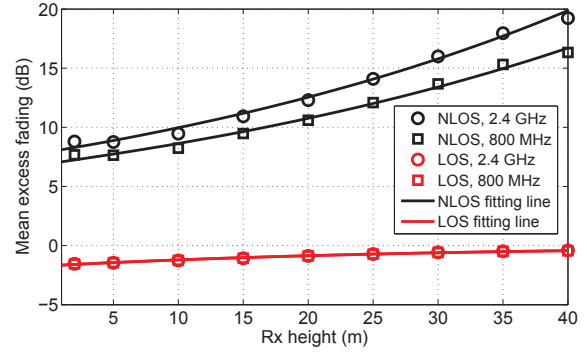

Fig. 4. Mean excess fading for the EL model as a function of RX height in a dense urban scenario.

Fig. 5. STD of excess fading for the EL model as a function of elevation angle in a dense urban scenario.

system. Typically, the excess fading loss (EL) model is used to estimate the pathloss of large propagation distance in free space, with an addition of fading resulted from surroundings and terrain elevations, which satisfies the A2A channel in urban scenario.

A. Excess fading loss model

The EL model with free space pathloss $FSPL(d)$ can be expressed as [8]

$$PL_\xi(d, h_T, h_R) = FSPL(d) + \eta_\xi \qquad (4)$$

where

$$FSPL(d) = 20 \log_{10}(\frac{4\pi f d}{c}) \qquad (5)$$

with c, f, and d representing the speed of light, frequency, and propagation distance, respectively. The elevation angle is calculated as $\theta = \arcsin((h_T - h_R)/d)$. The excess loss is in normal distribution as $\eta_\xi \sim N(\mu_\xi, \chi_\xi^2)$, and $\xi = \{LOS, NLOS\}$. The mean μ_ξ and standard derivation (STD) χ_ξ are characterized as the function of altitude and elevation angle in the LOS and NLOS scenario, respectively.

As depicted in Fig. 3, it is observed that the excess fading falls into two types: LOS data marked by red circle and NLOS data marked by black circle. Compared to the NLOS part, the LOS part suffers from less excess fading. The mean excess fading is estimated in different RX height, and the STD shows a strong relation with the elevation angle. It can be noticed from Fig. 4 that the mean excess fading tends to increase with an increase in RX height. Because the higher the altitude is, there is less probability to benefit from the reflection and diffraction. The mean of NLOS part with frequency of 800 MHz is less than that of 2.4 GHz, since the signal with longer wave length suffers from less reflected and diffracted loss. The mean of LOS part is about -0.9 dB in dense urban scenario, which is caused by the wave guide effect. The regression can be expressed as

$$\mu_{LOS} = a_1 \exp(b_1 \cdot h_R) \qquad (6)$$

$$\mu_{NLOS} = a_2 \exp(b_2 \cdot h_R) \qquad (7)$$

Note that the mean of LOS part can be assumed to be constant for simplicity.

In dense urban scenario with frequency of 2.4 GHz, the STD of NLOS part is estimated within range from 8.0 dB to 9.6 dB in different RX height, but degrading from 11 dB to 2 dB with the elevation angle from $10°$ to $80°$. Fig. 5 depicts the fitting function of LOS and NLOS part as red and black curve, respectively. Similarly, the less the carrier frequency is, there is less shadow fading resulting from reflection and diffraction. The STD degrades with the increase of elevation angle as shown by the following functions:

$$\chi_{LOS} = a_3\theta + b_3 \qquad (8)$$

$$\chi_{NLOS} = a_4(\theta - b_4)^2 + c_4 \qquad (9)$$

This is because the propagation link with small elevation angle is more likely to undergo shadow fading from buildings. The fitting parameters for EL model are summarized in Table II, and the scenario1 and scenario2 are within the frequency of 800 MHz and 2.4 GHz, respectively.

B. Close-in free space reference distance model

Typically, the large-scale fading is characterized as the statistics such as PLE and shadow fading variance. Considering the reasonable accuracy and simplicity across many scenarios and frequency band [12] [13], the close-in (CI) free space reference distance model is also investigated in this paper. Note that an alternative to the CI model is the floating intercept (FI), or *alpha-beta* model, but the additional variation in intercept
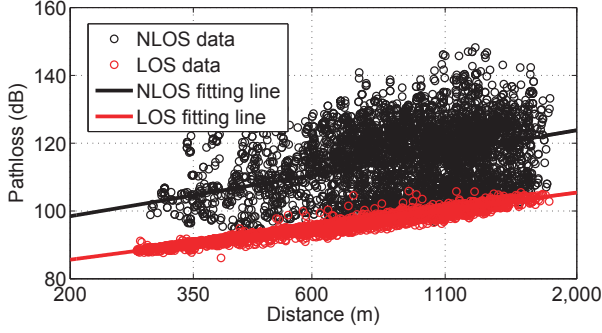
Fig. 6. Pathloss for the CI model in a dense urban scenario (RX = 30 m, f = 2.4 GHz).
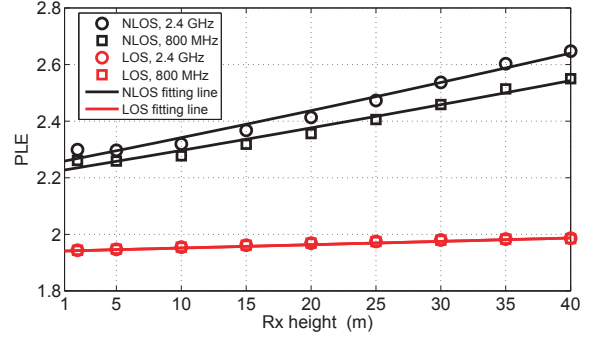

Fig. 7. PLE for the CI model as a function of RX height in a dense urban scenario.

Fig. 8. CDF of pathloss in a dense urban scenario in the LOS and NLOS environments (f = 2.4 GHz).

adds the model complexity. The CI model with reference distance d_0 can be expressed as [12]

$$PL_\xi(d, h_T, h_R) = 10n_\xi \cdot \log_{10}(d/d_0) + FSPL(d_0) + X_{\sigma_\xi} \tag{10}$$

The model uses the d_0 (e.g., 1 m) as the FSPL anchor point, to obtain the variation in the PLE n_ξ, which is dependent on the propagation condition. X_{σ_ξ} is the shadow fading in lognormal distribution with a STD of σ_ξ, and $\xi = \{LOS, NLOS\}$.

Fig. 6 depicts the pathloss at the RX height of 30 m with the frequency of 2.4 GHz, and there is clear difference between the LOS data and NLOS data. With the minimum mean square error (MMSE) method, the PLE of LOS part is estimated as 1.98 and the STD of shadow fading is 0.9 dB, whereas the corresponding estimates for NLOS part is 2.54 and 9.43 dB. Fig. 7 depicts the height dependent behavior of PLE, on the one hand, the PLE of LOS part is nearly but less than 2 due to wave guide effect, on the other hand, the PLE of NLOS part increases with an increase in RX height, resulting from less probability of receiving any reflected rays and hence degrading the wave guide effect. Another finding is that the benefit in reflection and diffraction leads to decay in PLE within less carrier frequency. It is also worth mentioning that the STD expresses the similar behavior as the EL model.

Considering the trade-off between simplicity and accuracy, the PLE and STD are associated with the RX height and elevation angle as

$$\begin{cases} n_{LOS} = \tilde{a_1}\exp(\tilde{b_1} \cdot h_R) \\ n_{NLOS} = \tilde{a_2}\exp(\tilde{b_2} \cdot h_R) \\ \sigma_{LOS} = \tilde{a_3}\theta + \tilde{b_3} \\ \sigma_{NLOS} = \tilde{a_4}(\theta - \tilde{b_4})^2 + \tilde{c_4} \end{cases} \tag{11}$$

where the fitting parameters are summarized in Table III. Note that the n_{LOS} can be approximated as 2 for simplicity. To validate the proposed parameters in EL and CI model, the simulation is performed at different heights in dense urban scenario. It is observed in Fig. 8 that the fitting results show good approximation with the raw simulated data. The variation in the cumulative distribution function (CDF) plot with respect to the height also implies the increase of mean excess fading and PLE with the altitude.
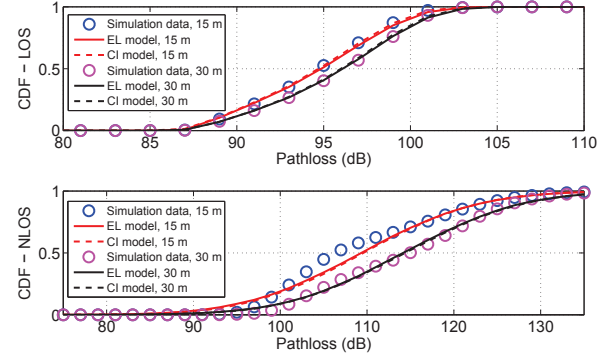
IV. LOS PROBABILITY

Considering the difference of channel behavior in the LOS and NLOS environment, the LOS probability plays an important role in the channel modeling. In the 3GPP standards, the LOS probability degrades exponentially with an increase in the link length, and the height of base station is negligible [14]. Based on the ray-tracing simulation, simple empirical formula is derived with respect to the elevation angle in the A2G channel [15]. However, the LOS probability is also correlated to the altitude in the A2A channel, in particular for the RX height. With the geometrical deployment of buildings, an approximate expression of LOS probability is derived as

$$\rho_{LOS}(h_R, \theta) \approx \exp(-\kappa Q(\frac{h_R}{\gamma})\cot(\theta)) \tag{12}$$

where $\kappa = 4\gamma\sqrt{2\alpha\beta/\pi}$ denotes the decay factor associated with the empirical parameters in ITU-R model, indicating that the LOS probability relies on the distribution of buildings. $Q(\cdot)$ is the Q-function.

The proof of Eq. (12) is given as follows. The centers of buildings are assumed to follow a two-dimensional Poisson point process (PPP), and the number of buildings between TX and RX is a Poisson random variable with mean λ [14], which is dependent on the scenario. Conditioning on the k buildings distributed on the link of TX and RX with the probability
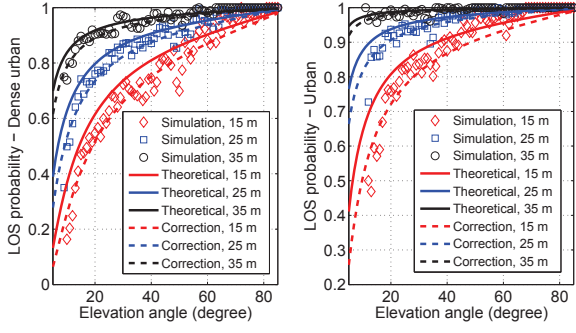
Fig. 9. LOS probability as a function of RX height and elevation angle in different scenarios.

$p(k)$, the expectation of LOS probability is calculated as

$$\rho_{LOS} = \sum_k \rho(LOS|k)p(k)$$
$$\overset{(a)}{=} \sum_k \rho(LOS|1)^k p(k)$$
$$\overset{(b)}{=} \sum_k \rho_0^k (\frac{\lambda^k}{k!}e^{-\lambda}) \qquad (13)$$
$$= e^{-\lambda} \sum_k \frac{(p_0\lambda)^k}{k!}$$
$$= e^{-\lambda(1-\rho_0)}$$

where (a) follows because the impact of each building on the LOS probability is independent. (b) follows from the Poisson distribution of k, and $\rho_0 = \rho(LOS|1)$ denotes the conditional LOS probability with one building. According to Theorem 3 in [14], ρ_0 can be further derived as

$$\rho_0 = \int_0^R F_h(h < h_B) \cdot \frac{1}{R} dx$$
$$\overset{(c)}{=} \frac{1}{R} \int_0^R [1 - \exp(-\frac{h_B^2}{2\gamma^2})] dx$$
$$= 1 - \frac{1}{R} \int_0^R \exp[-\frac{(h_R + \frac{h_T - h_R}{R}x)^2}{2\gamma^2}] dx \qquad (14)$$
$$= 1 - \frac{\sqrt{2\pi}\gamma}{h_T - h_R}[Q(\frac{h_R}{\gamma}) - Q(\frac{h_T}{\gamma})]$$

where F_h is the CDF of h, R is the horizontal distance between TX and RX, (c) follows from the Rayleigh distribution of building height, and h_B denotes the least height to block the LOS path. Note that the building is assumed to be uniformly distributed on the spacing $[0, R]$. According to Theorem 1 in [14], the mean λ can be derived as,

$$\lambda = \frac{2\beta(W + W)}{\pi}R + \beta W^2 = \frac{4\sqrt{\alpha\beta}}{\pi}R + \alpha \qquad (15)$$

where W is the width of square building. Plugging (14) and

TABLE II
FITTING PARAMETERS FOR THE EL MODEL.

Item	Dense urban1	Dense urban2	Urban1	Urban2
a_1, b_1	-1.70,-0.034	-1.72,-0.035	-1.12,-0.033	-1.15,-0.037
a_2, b_2	6.93,0.022	7.92,0.023	7.47,0.019	8.76,0.019
a_3, b_3	-0.016,1.80	-0.015,1.63	-0.015,1.60	-0.013,1.37
a_4	-0.0013	-0.0014	-0.0015	-0.0013
b_4, c_4	10,8.87	10,10.42	20,7.87	20,9.38

TABLE III
FITTING PARAMETERS FOR THE CI MODEL.

Item	Dense urban1	Dense urban2	Urban1	Urban2
$\tilde{a_1}, \tilde{b_1}$	1.94,0.0006	1.94,0.0006	1.96,0.0004	1.96,0.0004
$\tilde{a_2}, \tilde{b_2}$	2.22,0.0034	2.25,0.0040	2.23,0.0033	2.27,0.0039
$\tilde{a_3}, \tilde{b_3}$	-0.01,1.69	-0.01,1.48	-0.01,1.43	-0.01,1.21
$\tilde{a_4}$	-0.0011	-0.0012	-0.0015	-0.0016
$\tilde{b_4}, \tilde{c_4}$	10,8.48	10,9.96	20,7.63	20,9.11

(15) into (13) gives

$$\rho_{LOS} = \exp[-(\frac{4\sqrt{\alpha\beta}}{\pi}R + \alpha)\frac{\sqrt{2\pi}\gamma}{h_T - h_R}(Q(\frac{h_R}{\gamma}) - Q(\frac{h_T}{\gamma}))]$$
$$\overset{(d)}{\approx} \exp[-(\frac{4\sqrt{\alpha\beta}}{\pi}R + \alpha)\frac{\sqrt{2\pi}\gamma}{R\tan(\theta)}Q(\frac{h_R}{\gamma})]$$
$$\overset{(e)}{\approx} \exp[-4\sqrt{\frac{2\alpha\beta}{\pi}}\gamma Q(\frac{h_R}{\gamma})\cot(\theta)]$$

(16)

where (d) follows from the relationship $h_T - h_R = R\tan(\theta)$ and the approximating with high TX altitude (e.g., 300 m). (e) follows from the approximating in the case of long horizontal distance, and the proof of (12) is complete.

Fig. 9 shows the LOS probability in different scenarios, indicating that the denser the scenario is, the lower the RX height is, the propagation path is more likely to be blocked by the buildings. It is observed that the theoretical result matches the simulation data well, but the large elevation angle worsens the approximation due to short horizontal distance. In order to improve the performance, the MMSE method is used to obtain the corrected decay factor κ, in which the corresponding factor is adjusted from (0.59,0.78) to (0.75,1.06) in urban and dense urban scenario, respectively. Hence, the corrected decay factor is a little larger than the theoretical number.

V. MODEL IMPLEMENTATION AND VERIFICATION

The framework of implementation is illustrated as below, and the simulation area can be the small patch areas or their combination. Note that the TX and RX are assumed to be isotropic in the proposed guideline, whereas the antenna pattern should be considered when implementing the complete system design. The proposed A2A channel model simplifies the simulation calculation, and the implementation time can be shorten to several minutes. In order to verify the proposed

Algorithm 1 Framework of model implementation.

Require: The scenario, dense urban / urban; The center frequency, $f = 2.4$ GHz / 800 MHz; The TX altitude, $h_T \geq 200$ m; The RX altitude, $h_R \leq 40$ m;

Ensure: Pathloss, $PL(d, h_T, h_R)$;

1: Selecting the positions for TX and RX;
2: Calculating the distance d and elevation angle θ;
3: Calculating the LOS probability ρ_{LOS} according to (12);
4: Generating a random number in uniform distribution as $\omega \sim U[0, 1]$, if $\rho_{LOS} > \omega$, the propagation state is NLOS otherwise it is LOS;
5: Calculating the excess loss η, PLE n and STD σ of LOS or NLOS according to (6)-(9)(11);
6: Calculating the pathloss according to (4)(10) and repeating the above steps to obtain more data.

Fig. 11. CDFs of pathloss in a urban scenarios with different heights (TX = 300 m, f = 800 MHz).

REFERENCES

[1] Y. Zeng, R. Zhang, and T. J. Lim, "Wireless communications with unmanned aerial vehicles: opportunities and challenges," *IEEE Commun. Mag.*, vol. 54, no. 5, pp. 36-42, May 2016.

[2] M. Mozaffari, et al., "Unmanned Aerial Vehicle With Underlaid Device-to-Device Communications: Performance and Tradeoffs," *IEEE Trans. on Wireless Comm.*, vol. 15, no. 6, pp. 3949-3963, Jun. 2016.

[3] C. Zhang and W. Zhang, "Spectrum Sharing for Drone Networks," *IEEE J. Sel. Areas Commun.*, vol. 35, no. 1, pp. 136-144, Jan. 2017.

[4] L. Zhou, Z. Yang, S. Zhou and W. Zhang, "Coverage Probability Analysis of UAV Cellular Networks in Urban Environments," *IEEE International Conference on Communications Workshops*, pp. 1-6, 2018.

[5] N. Ahmed, S. S. Kanhere, and S. Jha, "On the importance of link characterization for aerial wireless sensor networks," *IEEE Commun. Mag.*, vol. 54, no. 5, pp. 52-57, May 2016.

[6] A. Rafhael, et al., "Radio Channel Modeling for UAV Communication Over Cellular Networks," *IEEE Wireless Commun. Lett.*, vol. 6, no. 4, pp. 514-517, Aug. 2017.

[7] Z. Yang, L. Zhou, G. Zhao and S. Zhou, "Channel Model in the Urban Environment for Unmanned Aerial Vehicle Communications," *accepted by the European Conference on Antennas and Propagation*, 2018.

[8] A. Al-Hourani, S. Kandeepan, and A. Jamalipour, "Modeling air-to-ground path loss for low altitude platforms in urban environments," *IEEE Global Communications Conference*, pp. 2898-2904, 2014.

[9] P. Mededovic, M. Veletic, and Z. Blagojevic, "Wireless insite software verification via analysis and comparison of simulation and measurement results," *Proceedings of the 35th International Convention MIPRO*, pp. 776-781, 2012.

[10] ITU-R, "Rec. P.1410-2 Propagation Data and Prediction Methods for The Design of Terrestrial Broadband Millimetric Aadio Access Systems," *P Series, Radiowave propagation*, 2003.

[11] V. S. Abhayawardhana, I. J. Wassell, D. Crosby, M. P. Sellers, M. G. Brown, "Comparison of empirical propagation path loss models for fixed wireless access systems," *IEEE Vehicular Technology Conference*, vol. 1, pp.73-77, 2005.

[12] T. S. Rappaport, G. R. MacCartney, M. K. Samimi, and S. Sun, "Wideband Millimeter-Wave Propagation Measurements and Channel Models for Future Wireless Communication System Design," *IEEE Trans. on Wireless Comm.*, vol. 63, no. 9, pp. 3029-3056, Sep. 2015.

[13] L. Zhou, et al., "Path loss model based on cluster at 28 GHz in the indoor and outdoor environments," *Science China Information Sciences*, vol. 60, no. 8, pp. 080302:1-080302:11, August 2017.

[14] T. Bai, R. Vaze, and R. W. Heath, "Analysis of Blockage Effects on Urban Cellular Networks," *IEEE Trans. on Wireless Comm.*, vol. 13, no. 9, pp. 5070-5083, Aug. 2014.

[15] J. Holis and P. Pechac, "Elevation dependent shadowing model for mobile communications via high altitude platforms in built-up areas," *IEEE Trans. Antennas Propag.*, vol. 56, no. 4, pp. 1078-1084, April 2008.
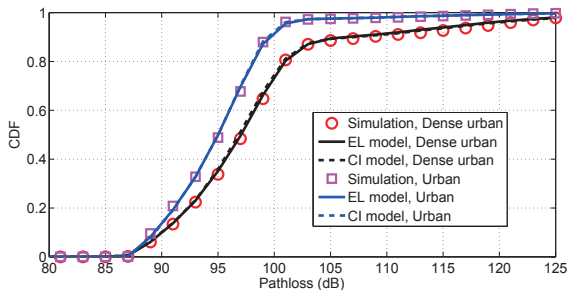
Fig. 10. CDFs of pathloss for different scenarios (TX = 300 m, RX = 30 m, f = 2.4 GHz).

model, we compared the raw data from ray-tracing simulator versus the simulation result. Fig. 10 and Fig. 11 depict the comparison in different scenarios and heights, respectively. On the one hand, the proposed model is suitable for different urban scenarios with respect to ITU-R model. On the other hand, the denser deployment of building and lower RX height degrade the pathloss due to less LOS probability. Moreover, the CI model and EL model can be used interchangeably because of the similar performance and complexity.

VI. CONCLUSIONS

Based on the conventional EL and CI models, this paper has investigated the relationship between the large-scale fading statistics and environmental setups in A2A channels. The PLE and mean excess fading increase with an increase of RX height, and the STD of shadow fading is characterized as a negative function of elevation angle. The approximate formula of LOS probability has been derived and it is associated with both the RX height and elevation angle with the assumption of high TX height. The parameterization and implementation of the proposed model can serve as a simple tool for UAV system-level estimations, which can easily be extended to different urban scenarios. Further UAV channel measurements should be taken to extract more realistic model parameters.

ACKNOWLEDGEMENT